A MONTE CARLO PARTICLE STUDY OF A SEMICONDUCTOR RESPONDING TO A LIGHT PULSE

C Moglestue

GEC Research Laboratories
Hirst Research Centre
Wembley Middlesex UK

ABSTRACT

A picosecond photodetector has been simulated by means of the Monte Carlo particle model. The detector consists of a 2 µm film of n-type GaAs, doped uniformly with 10^{22} donors m^{-3}. The film is covered with metal strips 2 µm apart. Every second strip is equally biased, the others earthed. The simulated response to a femtosecond flash is a current which peaks after about 1 ps, and dies down within 10 ps. No current is observed for biases below a threshold of 1V. This device promises therefore to be operable for pulses at frequencies up to 100 GHz.

The flash generates a stationary electron-hole plasma, only a few carriers escape to form the response current pulse. The remainder of the plasma will eventually be eliminated by recombination

1 INTRODUCTION

With the steady advance in the introduction of optical fibres for communication in the mm-wave band the attention of researchers and engineers has turned towards finding a fast photodetector, a device that transforms the light pulse at the receiving end into an electric signal that can be processed by the electronic circuit there. Beneking [1,2] has reviewed the theory for photodetectors, assuming that the electrons and the holes produced by the light immediately separate and find their way to the anode and cathode, respectively, guided by the local electric field. All particles will be absorbed by the terminals except those recombining at the surface of the semiconductor. Gammel et al [3] have manufactured such a detector, known as an OPFET, which has a response time of the order of tens of picoseconds. They applied a light pulse of length 15 ps, the OPFET responded with a current pulse peaking after approximately 50 ps and decaying after another 50 ps.

On the other hand, it has been shown by means of Raman spectroscopy that a light pulse creates an electron-hole plasma that survives for much longer intervals of time, at least up to 400 ps after the light was turned off [4,5]. The particles of the plasma interact with all the other particles within the screening distance through mutual Coulomb fields that keep the plasma together.

To resolve this problem, we have simulated a single photodetector using the Monte Carlo particle model [8] which is three dimensional in momentum space. We have favoured this over relaxation models because there is no thermal equilibrium in the plasma, it is concerned with individual particles, and the method gives a profound microscopic insight into the dynamics of the particles which are present in the device.

This method, which will be described briefly in Section 3, consists of following the transport histories of individual electrons and holes in detail. In Section 4 we demonstrate that the response signal is similar to that observed by Gammel et al, [3] comes about 1 ps after the infinitely short flash, and lasts for a time of the order of picoseconds. Our device therefore promises to be able to handle signals of frequencies up to 100 GHz.

2. THE DETECTOR

The photodetector consists of a uniformly n-type doped GaAs film, 2 μm thick, covered with parallel metal strips, 2 μm apart. Every second strip is earthed, the others are biased at voltage V. The substrate on which the film sits reflects electrons but is perfectly transparent to the light. The metal is perfectly opaque, the film is doped at 10^{22} donors m^{-3}. Figure 1 shows the part of the detector simulated. The results

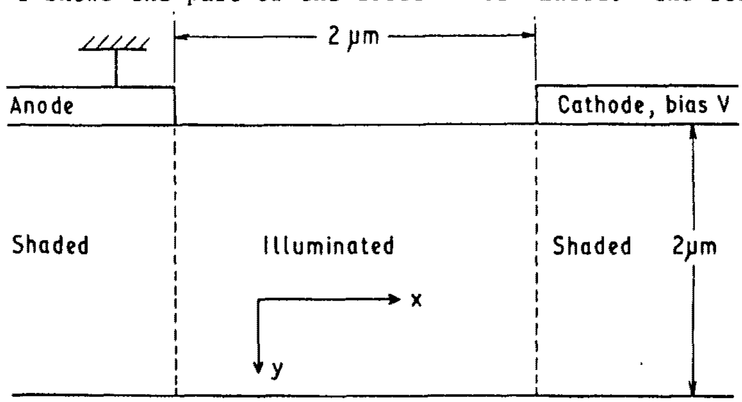

Fig 1: The GaAs photodetector geometry. The anode is earthed, the cathode biased. The coordinate system referred to in Eq. 9 is indicated here

obtained for this part apply throughout the rest of the detector by virtue of its symmetry.

3 SIMULATION

The Monte Carlo particle method represents an indirect way of simultaneously solving

(i) Poisson's field equation

$$\nabla^2\phi = \rho(\underline{r})/\varepsilon\varepsilon_o \qquad (1)$$

where ϕ represents the electric potential, ρ the position ($\underline{r}$) dependent charge density and $\varepsilon\varepsilon_o$ the absolute permittivity, and

(ii) Boltzmann's transport equation

$$\hbar\underline{k}\cdot\nabla f_k/m^* + q\underline{E}\nabla_k f_k/\hbar = \int\{f_k(1-f_k) - f_{k'}(1-f_k)\}W(\underline{k},\underline{k}')d^3\underline{k}' \qquad (2)$$

Here m^* and q represent the effective mass and the charge of the particle respectively, $\underline{k}$ and $\underline{k}'$ the wave vector before and after an interaction with the lattice, and f_k the distribution function which measures the number of carriers in state $\underline{k}$ at the position $\underline{r}$. W represents the probability per unit time that the carrier is transferred from state $\underline{k}$ to state $\underline{k}'$ anywhere in the crystal on interaction with the lattice. The integration is carried out over all $\underline{k}'$. We make no initial assumptions regarding the shape of f_k; the correct forms will emerge from the calculations. The expressions for W have been obtained from quantum theory [9]. The processes included here are acoustic and optical phonons, phonons causing transfer between various energy bands and scattering from ionised impurities. Creation of hole-electron pairs through avalanche in strong electric fields has also been included in the model as an option. Processes with scattering rates orders of magnitude lower than for the principal acoustic ones, such as capture and release of trapped carriers, recombination of hole-electron pairs etc, are not considered here as they contribute insignificantly during the part of the life of the detector being studied. The trapping and release rates are of the order of nanoseconds or longer [10]. The model includes three conduction bands: the Γ,X and Δ valleys, and three valence bands: the light, heavy and split-off band.

We follow the transport of individual particles. The probability that the particle will fly freely for a time t since it was last scattered is

$$g(t)dt = \Gamma[\underline{k}(t)] \exp\left(-\int_0^t \Gamma[\underline{k}(t')]dt'\right)dt \qquad (3)$$

where g(t) represents the probability density of scattering at time t, and $\Gamma[\underline{k}(t)]$ represents the sum of all rates from the individual types of scattering mechanisms, $\Gamma_s[\underline{k}(t)]$, where

$$\Gamma_s[\underline{k}(t)] = \int W_s(\underline{k},\underline{k}')d\underline{k}' \tag{4}$$

and $W = \sum_s W_s$. The individual flight times are chosen by means of a random number of the same distribution g(t). The subsequent scattering mechanism is chosen by another random number r_σ with a uniform distribution between 0 and $\Gamma[\underline{k}(t)]$ such as

$$\sum_{s=1}^{S'} \Gamma_s < r_\sigma < \sum_{s=1}^{S'+1} \Gamma_s \tag{5}$$

where $S'=0,1,\ldots,$ $S'=0$ indicating that the sum of the left side is zero. The chosen scattering mechanism is the one which has the number S'satisfying (5). Furthermore, two additional random numbers r_ϕ and r_Θ with the distribution

$$|\langle k|H(\phi,\Theta)|k'\rangle|^2 \tag{6}$$

define the scattering angles ϕ and Θ. H is the Hamiltonian for transfer from $\underline{k}$ to $\underline{k}'$.

Each particle is followed for a set time, δT, known as the field adjusting time step, which is of the order of femtoseconds. The Poisson equation (1) is then solved, when $q(\underline{r})$ consists of the static doping charge and the mobile carriers. We use Hockney's FACR algorithm [11] subject to the boundary conditions defined by the bias at the terminals to solve (1). This requires that the area of solution is divided into a rectangular mesh of sides h_x and h_y. Any variation in the third (z) dimension in Eq(1) perpendicular to the plane of Figure 1 is neglected. During free flight the field pattern obtained from Eq(1) stays frozen, but is updated for each field adjusting time step. The error thus made is negligible provided δT is chosen sufficiently small. The solution is repeated every δT, even during the steady state.

The size of the population we follow is restricted by the limitations in speed and memory of the computer, but a representative size is 10000 individuals. Each particle of this subpopulation therefore, referred to as a super particle below, represents a charge

$$e = h_x H_y Z n q / \nu \tag{7}$$

for the purpose of estimating the currents and for solving Eg(1) only, ν is the number of super particles needed to create charge neutrality, n is the number density of the donors and Z is the width of the semiconductor in the z-direction. Z is normalised to 1 metre, and so are our results too.

As our model is a stochastic one, it is also well suited to study noise phenomena.

A single flash of light is shone into the device for a duration less than δT. That part of the flux absorbed by the device, ϕ, generates

$$n_{ph} = \phi Z \nu / (An) \tag{8}$$

pairs of super electron-holes, each constituent will have zero energy and momentum, corresponding to light of energy equal to that of the band-gap. Here A represents the area of the exposed surface (no light penetrates the electrodes). The electron-hole pair distribution has a uniform x-component and a y-component varying according to

$$y = t\left[1-\exp(^{-t}\gamma r_y)\right] \left[1-\exp(-\gamma t)\right]^1 \tag{9}$$

due to attenuation of the light from absorption. The film thickness is t, and γ is the absorption coefficient chosen here to be 10^6 m^{-1}, which is near the value quoted for GaAs [2].

The total charge generated by the light flash is zero. Although Coulomb interaction between individual particles can be disregarded, the collective interaction of one particle with all the other ones has been included in Eq (1), and represents the Hartree-Fock one-particle approximation.

4 RESULTS AND DISCUSSION

The simulation starts with the dark current. At time 0, when the flash is applied, simulation has been going on for

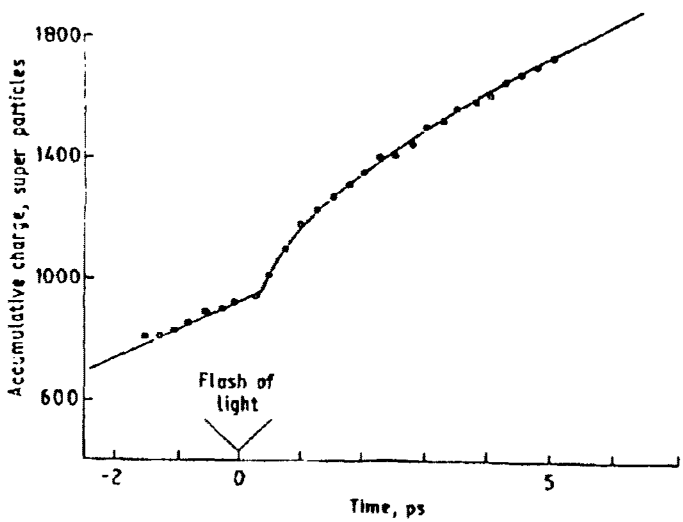

Fig 2: Accumulative super particles count at the cathode vs time. Each super particle represents a charge given by Eq.(7). The flash is applied at time 0.

sufficiently long time to establish the dark current value with sufficient accuracy. The current is obtained by counting the charges absorbed by a terminal, Figure 2.

The response to the flash is a current pulse that reaches its peak after 1 to 2 ps. Within 5 ps the current has decayed to its dark value, Figure 3. The delay in response is due to the time of transit of electrons to reach the anode. This behaviour has also been observed by Gammel and Ballantyne [3] and Platte [13]. Figure 4 shows that the ratio of the peak and the dark current rises with increased bias, and no pulse is formed for biasses below 1V.

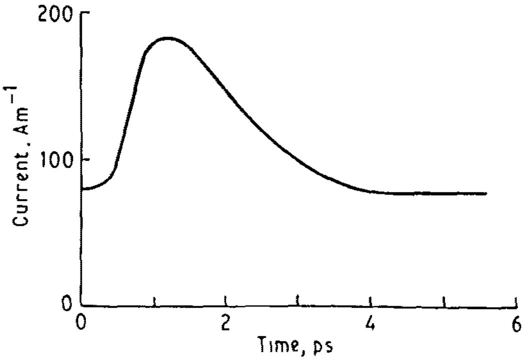

Fig 3: Cathode current vs time. It is obtained from the slope of the curve of Fig 2. The flash is applied at time 0.

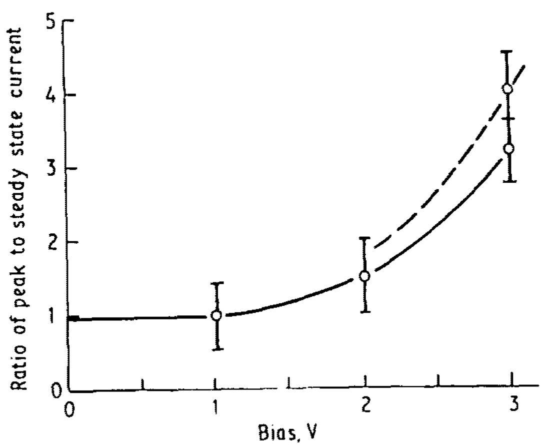

Fig 4: Ratio of peak and dark current vs applied bias.
___ No avalanche multiplication
--- With avalanche multiplication
Error bars indicate accuracy of simulation

Figure 5 shows that most of the holes and the electrons generated by the light pulse still remain in the semiconductor. They form a stationary electron-hole plasma. Only a small fraction of the carriers reach the electrodes and only those nearest to the electrode will contribute to the current pulse.

Although the total charge represented by the plasma is zero, it is held together by electrostatic attraction. If one particle tries to leave the plasma cloud, the excess opposite charge it would leave behind would pull it back. The plasma does not affect the dark current flowing when the response has decayed as this flows unobstructed by injecting electrons at the cathode and absorbing them at the anode.

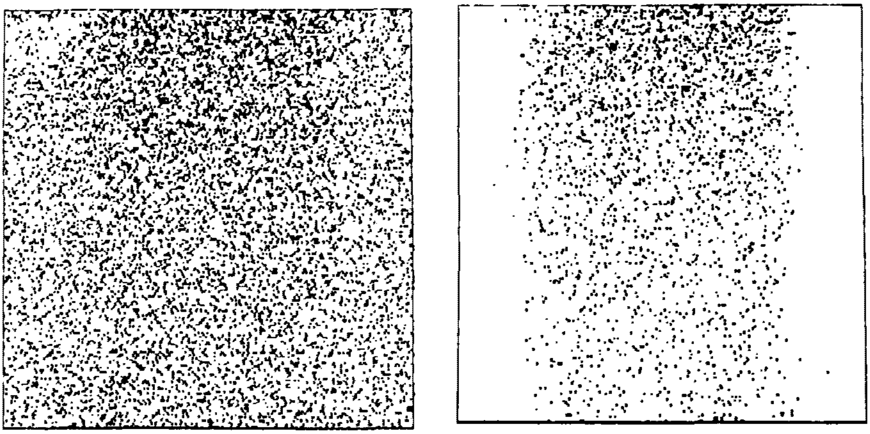

(a) (b)

Fig 5: Momentary positions of (a) electrons and (b) holes in the photodetector

Screening forms within the plasma within the first picosecond [12]. This means that there is a limited extent to the Coulombic forces between the particles. Long after the termination of the simulation, of the order of nanoseconds, recombination starts, paired with emission of both phonons and photons. The latter will not cause any significant additional currents through reabsorption.

We have repeated the simulation for 3V bias, allowing electron-hole pairs to form through impact ionisation right from the start, i.e. even during the dark current stage prior to the flash. Up till time t=0 no such pairs were formed, but after the flash we got impact ionisation. The rate of this peaked after 750 fs, figure 6, and died down slowly. After 10 ps there was still some plasma formed by this process. This results in an increased pulse length, dashed curve Figure 4, with a prolonged tail, Figure 7. The impact ionisation starts in a small area of the cathode, very near to the surface. As the activity diminishes, this area spreads downwards, and is limited to the cathode side of the plasma.

In our computer model we have used super particles instead of real particles for the purpose of estimating the local electric fields. This means that we are dealing with large point charges generating large dipole fields extending over

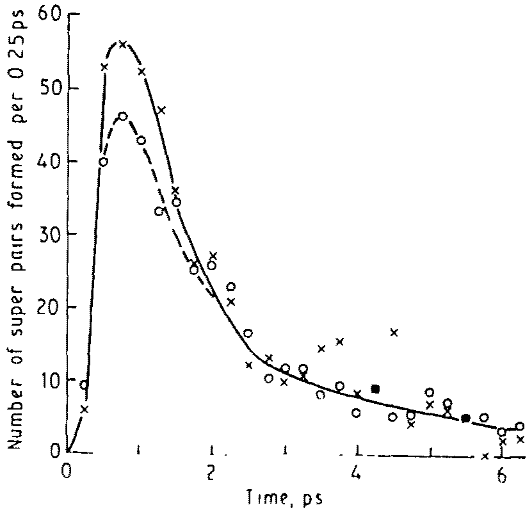

Fig 6: Number of electron-hole pairs created in intervals of 25 ps vs time for 3V bias (__X__) and the same bias with four times as many superparticles (--O--)

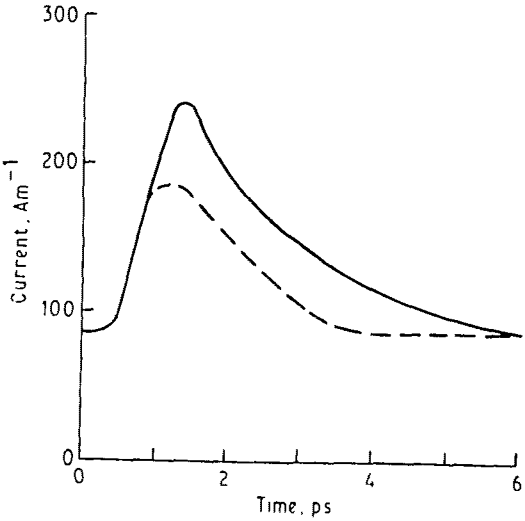

Fig 7: Cathode current vs time with and impact ionisation carrier multiplication (---) and with (___)

distances whose average is equal to the separation of the super particles. These dipole fields may be strong enough to give another particle near by sufficient energy to cause ionisation. In other words, our impact ionisation may partly be a computational artefact. With more super particles each one would represent correspondingly less charge, and form a correspondingly denser plasma. The dipole fields will still be the same, but their extent will be smaller, giving an adjacent particle less chance to be exposed sufficiently long to its influence to cause ionisation. To test this, the simulation was carried out once more with four times as many super particles. In Figure 6 the number of electron-hole pairs created in intervals of 0.25 ps is plotted against time for both of these simulations. The curve for the latter case has been normalised to the former by dividing by 4. Within the statistics of the sampling, there is no significant difference in the hole-electron generation rate through impact ionisation except at the peak. The effect is thus real and should be included in the simulation. At higher biases avalanche multiplication forms a significant part of the pulse signal.

The internal fields have been mapped. Prior to the application of the flash, a nearly stationary high field Gunn domain had formed underneath the anode. Most of the potential fall between the terminals takes place in this area. Here the electrons enter the higher energy conduction bands and become heavy. After the flash this domain starts to move downwards and towards the cathode as it weakens. The weakening of this domain, which never reaches the cathode, is correlated with the decay of the electric pulse. The domain is no longer visible when the current pulse is extinct.

5 CONCLUSION

A photodetector has been simulated using the Monte Carlo particle model. The geometry of the detector is like that of a transistor without a gate and a Gunn domain has formed. The area between the terminals is illuminated by a high intensity light flash of infinitely short duration. The response pulse reaches a maximum after about 1 ps and dies down a few picoseconds later. Below a threshold bias of about 1V no pulse is seen. The light causes a stationary electron-hole plasma to form in which more carriers are produced by impact ionisation at the anode side. The contribution to the response signal from the latter increases with increasing bias.

A photodetector of this design promises to be a fast device, and therefore has microwave applications. As the response pulse is extinct after less than 10 ps, such a device could be used as a high frequency converter of light to electric signals.

REFERENCES

1 BENEKING, H
'On the response behaviour of fast photoconductive optical planar and coaxial semiconductor devices'
IEEE Trans Electr. Devices ED-29 (9), pp 1430-1441, 1982

2 BENEKING, H.
'Gain and bandwidth of fast near-infrared photodetectors: a comparison of diodes, phototransistors and photoconductive devices'
ibid, pp 1420-1431

3 GAMMEL, J.C. and BALLANTYNE, I.M.
'The OPFET: a new high speed optical detector'
IEDM, pp 120-123, 1978

4 TANAKA, S., KOBAYASHI, H., SAITO, H. and SHIONOYA, S.
'Spantaneous luminescence due to high density electron-hole plasma in GaAs under nano-and picosecond pulse excitation'
Solid St. Comm. 33, pp 167-170, 1980

5 TANAKA, S., KUWATA, T., HOKIMOTO,T., KOBAYASHI, H. and SAITO, H.
'Picosecond dynamics of optical gain due to electron-hole plasma in GaAs under near band-gap excitation'
J. Phys. Soc. Japan 52, pp 677-685, 1983

6 ARYA, K. and HANKE, W.
'Many body Coulomb effects on the gain and absorption line shapes of the electron-hole plasma is GaAs'
Phys. Rev. B23, pp 2988-2994, 1981

7 ARYA, K. and HANKE, W.
'Coulomb effects on the gain and absorption spectra of the electron-hole plasma in GaAs'
Solid St. Comm. 33, pp 739-742, 1980

8 MOGLESTUE, C.
'Monte Carlo particle modelling of small semiconductor devices'
Comp. Meth. Appl. Mech. and Eng. 30, pp 173-208, 1982

9 JACOBONI, C. and REGGIANI, L.
'The Monte Carlo method for the solution of charge transport in semiconductors with applications to covalent materials'
Revs. Modern Physics 25 pp 645-705, 1983

10 MARTIN, G.H., MITONNEAU, A. and MIRCEA, A.
'Electron traps in bulk and epitaxial GaAs crystals'
Elect. Lett. 13, (7), pp 191-193, 1978

11 HOCKNEY, R.W.
'A fast direct solution of Poisson's equation using Fourier analysis'
J. Assoc. Comput. Mach. 12, pp 95-113, 1965

12 FUJIMOTO, J.G., SHEVEL, J.G. and IPPEN, E.P.
'Femtosecond time-resolved excition dynamics in CdSe'
Sol. St. Comm. 49, pp 605-609, 1984

13 PLATTE, W.
'Optoelectronic microwave switching via laser-induced plasma tapers in GaAs microstrip sections'
IEEE-MTT-29, pp 1010-1018, 1981